

Article

The Potential of Spectral Indices in Detecting Various Stages of Afforestation over the Loess Plateau Region of China

Jing Guo ^{1,2} and Peng Gong ^{1,2,*}

¹ Ministry of Education Key Laboratory for Earth System Modeling, Department of Earth System Science, Tsinghua University, Beijing 100084, China; guoj15@mails.tsinghua.edu.cn

² Joint Center for Global Change Studies, Beijing 100875, China

* Correspondence: penggong@tsinghua.edu.cn; Tel.: +86-010-62788023

Received: 7 August 2018; Accepted: 14 September 2018; Published: 18 September 2018



Abstract: China has the greatest afforestation area in the world, mainly due to the implementation of various ecological restoration projects, which have taken place over several decades. However, the progress of these restoration projects has rarely been evaluated through sapling growth monitoring. In this research, we assessed the potential of eighteen spectral indices derived from time-series Landsat data to characterize the different stages of afforestation over the Loess Plateau region. First, we obtained data for the afforestation area from 1997 to 2010. Then we estimated the average year of afforestation that could be uniquely identified and the sensitivity to growth exhibited by each of the indices. The results show that the first shortwave infrared band (SWIR1) of the Landsat Thematic Mapper and the Brightness index from the tasseled cap transformation (TCB) had the fastest response to sapling growth. It takes 4.2 and 4.3 years on average for the saplings to be detected as forest by SWIR1 and TCB, respectively. However, these two indices saturate too soon to allow better distinction of the various stages of sapling growth but are better for monitoring the over-reporting situation. By contrast, the disturbance index (DI), and the normalized burnt ratio (NBR) and the normalized burnt ratio 2 (NBR2) respond slowly to sapling growth and can detect forest at 7.4 years on average. Unlike SWIR1 and TCB, these indices do not saturate early and can provide more detail on the level and structural condition of sapling growth.

Keywords: Loess Plateau; sapling growth; spectral indices; Landsat

1. Introduction

Although a decline in forest-covered areas has occurred over several decades throughout the world [1], there has also been a decreasing trend of natural forest felling and the introduction of more man-made forests and conservation, due to the initiation of new forest policies [2]. In order to eradicate a series of environmental problems, such as soil erosion and desertification, China has implemented many ecological restoration projects and, as a result, China now has the largest afforestation area in the world [3,4]. With a large amount of investment and considerable national effort, these afforestation projects have increased vegetation coverage [5] and improved environmental conditions [6,7] in China. Because afforestation is a gradual process and it can take several years or decades for saplings to grow into forest, it is necessary to continuously monitor the process of sapling growth in order for forest managers and various other stakeholders to be well informed of the growth conditions of newly planted trees and their environmental impact, as well as the effectiveness of afforestation at different stages. Due to incomplete policies over the execution of compensation for afforestation projects and local demands for land for development, in some parts of the country forest plantation areas have been converted to other land-use types [8].

Therefore, continuous monitoring of afforestation is not only necessary for assessing the accomplishment and condition of plantation growth at different stages but is also a reliable source of information for consolidating achievements and forming suitable compensation policies. Although many methods have been proposed to obtain the actual distribution of afforestation at regional and national levels [9–11], little research has been done to monitor the process of sapling growth at various stages.

Landsat provides openly available remotely sensed data. It has the longest data archives at over 40 years, and analysis-ready production covering the entire world. In China, the greatest intensity of afforestation was carried out after the year 2000, and so the long time series provided by Landsat is a good choice for monitoring afforestation. In addition, time series Landsat images have been widely applied to monitor gradual and abrupt forest changes [12–14]. Most of these methods are based on the temporal trajectory of spectral indices (e.g., the normalized difference vegetation index, and tasseled cap indices) extracted from time series Landsat data. Even under the same circumstances, spectral indices can vary largely in their capacity for capturing and describing forest change dynamics [15–20]. Different spectral indices have different sensitivities to changes in green vegetation. Choosing a suitable index for monitoring different types of forest change can help to better describe the change dynamics. Some efforts have been made to study different spectral indices in Landsat time series for monitoring forest disturbance and recovery [15–20]. However, those studies have focused on forest disturbance and subsequent recovery, and the transition of forest between natural growth and disturbance. Little research has concentrated on afforestation implemented according to restoration policy, especially in places with sparse vegetation like China's Loess Plateau.

The objectives of this study are to compare eighteen spectral indices widely used in forest monitoring with Landsat time series data over a long period of time and to find their strengths and weaknesses in characterizing afforestation especially the process of sapling growth in afforestation over the Loess Plateau.

2. Study Area

The Loess Plateau is located in north-central China, and is one of many ecologically fragile regions in China vulnerable to soil erosion and other environmental problems. In 1999, the Grain for Green project, which converted cropland to forest land on steep slopes, was initiated to help eradicate these problems [21]. Currently, the Loess Plateau is one of the core regions for implementing ecological restoration projects. To serve the purposes of this study, we concentrated on the southeastern portion of the Loess Plateau where forest is the dominant land cover type [22,23] (Figure 1).

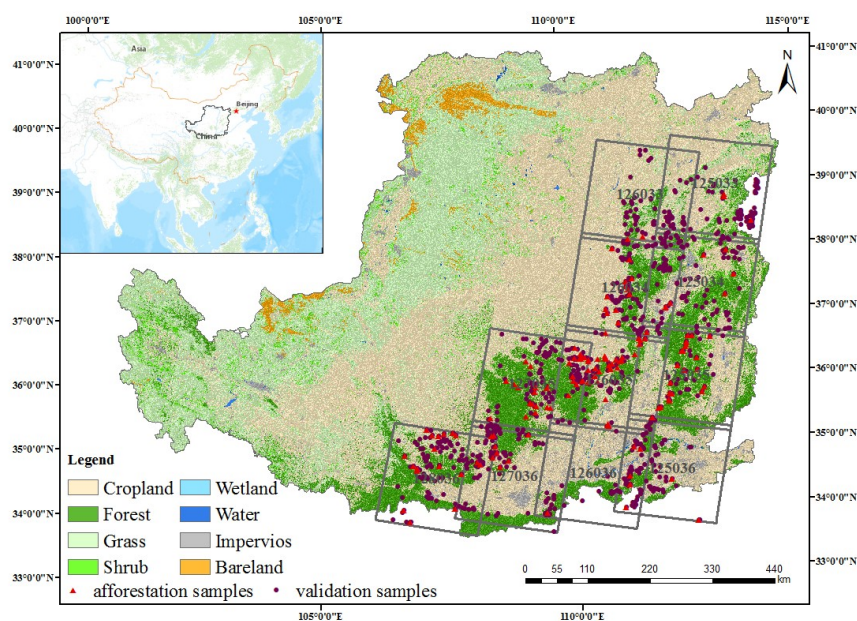


Figure 1. Area covered by frames of Landsat scenes chosen for this study.

3. Data and Method

3.1. Data

It required eleven Landsat scenes (path/row: 126/33, 125/33, 126/34, 125/34, 127/35, 126/35, 125/35, 128/36, 127/36, 126/36, 125/36) to cover the southeastern part of the Loess Plateau (Figure 1). Landsat Surface Reflectance Level-2 science products, downloaded from USGS (<https://earthexplorer.usgs.gov>), were used in this research. Due to the possible impacts caused by different spectral ranges and surface reflectance algorithms between Landsat 7 and 8 (<https://landsat.usgs.gov/landsat-surface-reflectance-data-products>), we chose only those scenes acquired by Landsat 5 and Landsat 7 during the growing season from June to September from 1997 to 2010 with less than 80% cloud cover to reduce seasonal effects. All Landsat Surface Reflectance Level-2 science products on the website had been atmospherically corrected using Ecosystem Disturbance Adaptive Processing System (LEDAPS), and include a cloud, shadow, water, and snow mask (<https://landsat.usgs.gov/landsat-surface-reflectance-data-products>). All images in the same year were mosaicked to generate one complete and cloud-free image per year from the time series Landsat images between 1997 and 2010 based on the best-available-pixel (BAP) composites method [24].

3.2. Spectral Indices Chosen for the Experiment

In this study, the criterion used to choose the experimental indices is that the index has been widely used in monitoring forest change dynamics with Landsat time series data [12]. All the indices summarized in the review paper around forest monitoring using Landsat time series data [12] have been chosen. In our study, eighteen indices (Table 1) were chosen.

We generated a time series of these eighteen spectral indices based on time series Landsat image stacks from 1997 to 2010. A Savitzky-Golay filter was applied to smooth these time series indices [25]. The typical afforestation curve characteristics displayed by each of the eighteen time series indices are shown in the following table (Table 1). These indices can be divided into two groups: in one group the values of the indices rise gradually and in the other they decrease gradually with the growth of forest plantation.

Table 1. Typical time-series curves of afforestation displayed by various indices.

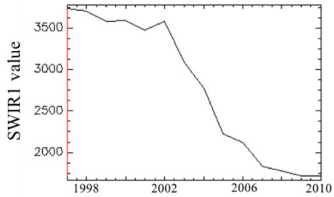
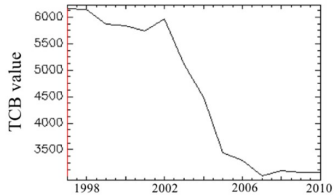
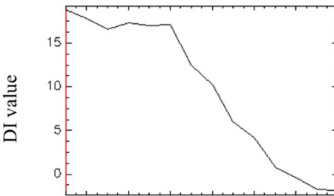
Indices	Description	Time-Series Curve of Afforestation
SWIR1	Short-wave infrared (1.55–1.75 μm) spectral range in micrometers [26]	
TCB	Tasseled Cap Brightness [27]	
DI	Disturbance Index [28]	

Table 1. Cont.

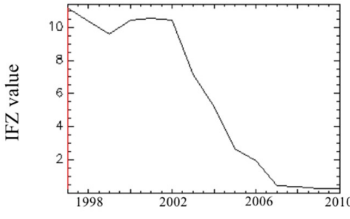
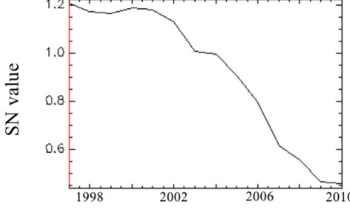
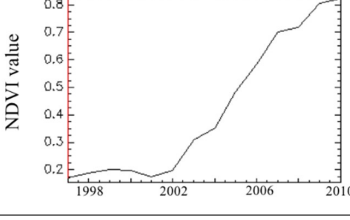
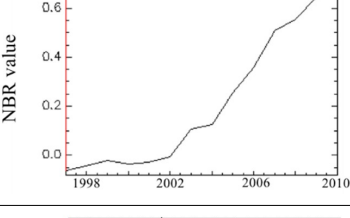
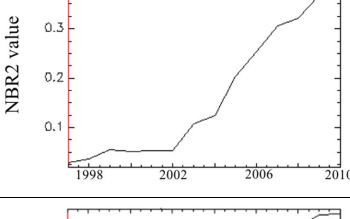
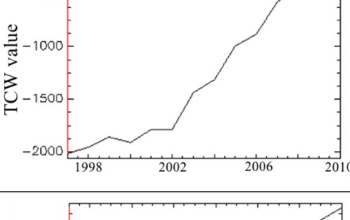
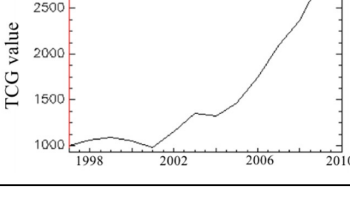
Indices	Description	Time-Series Curve of Afforestation
IFZ	Integrated Forest Z-score [29]	
SWIR/NIR (SN)	SWIR1/NIR ratio [30,31]	
NDVI	Normalized difference vegetation Index [9] $(NIR - RED)/(NIR + RED)$	
NBR	Normalized burned ratio $(NIR - SWIR2)/(NIR + SWIR2)$ [32]	
NBR2	Normalized burned ratio2 $(SWIR1 - SWIR2)/(SWIR1 + SWIR2)$ [33]	
TCW	Tasseled Cap Wetness [27]	
TCG	Tasseled Cap Greenness [27]	

Table 1. Cont.

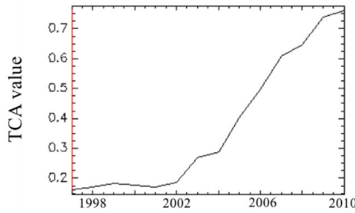
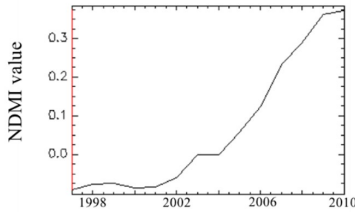
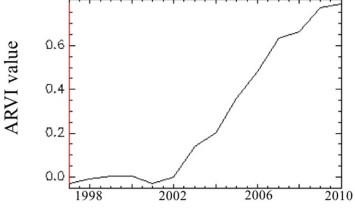
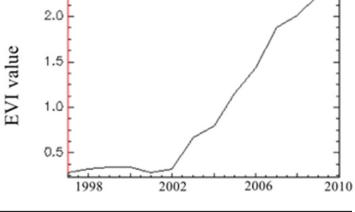
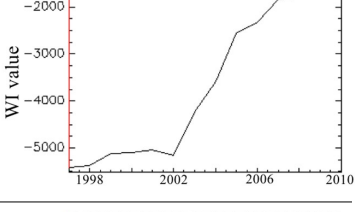
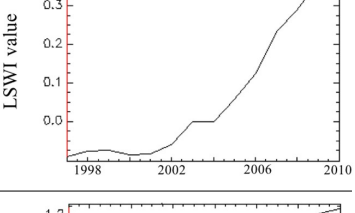
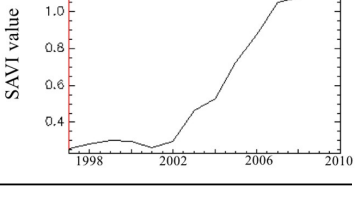
Indices	Description	Time-Series Curve of Afforestation
TCA	Tasseled Cap Angle [28]	
NDMI	Normalized difference moisture Index [34] $(NIR - SWIR1)/(NIR + SWIR1)$	
ARVI	Atmospherically Resistant Vegetation Index [35] $(NIR - (2RED - BLUE))/(NIR + (2RED - BLUE))$	
EVI	Enhanced Vegetation Index [36] $2.5(NIR - RED)/(NIR + 6RED - 7.5BLUE + 1)$	
WI	Woodiness Index [37] $512 - (RED + SWIR1)$	
LSWI	Land Surface Water [36] $(NIR - SWIR1)/(NIR + SWIR1)$	
SAVI	Soil Adjusted Vegetation Index [38] $(1 + 0.5)(NIR - RED)/(NIR + RED + 0.5)$	

Table 1. Cont.

Indices	Description	Time-Series Curve of Afforestation
WBDI	Wetness brightness difference index [39] WBDI = TCW – TCB	

3.3. Characteristics of an Ideal Sapling Growth Index Curve

During the process of plantation growth, different stages of saplings have different levels of ecological benefits based on their structural condition. The ability of soil and water conservation, carbon fixation, oxygen release, nutrient accumulation, and air purification functions can vary greatly between various sapling growth stages. Detailed information on the sapling growth process can help evaluate the ecological benefits more comprehensively. China’s afforestation policy usually provides subsidies to participating farmers or workers through local governments. As an example, the Grain for Green Project (GGP) offers 5- and 8-year subsidies for economic forest and ecological forest, respectively [40]. In 2014, the central government decided to provide subsidies in the first, third and fifth year after the year of plantation [41]. Therefore, it is vital to continuously monitor sapling growth to assess the effectiveness of afforestation. The amount and length of compensation can be altered based on the specific stage of sapling development and growth condition. An ideal index needs to provide more information at various stages of sapling growth and over a longer timespan to characterize the growth condition of forest plantation.

The time series curves of spectral indices chosen for the experiment all changed gradually. We took as an example an index that gradually rises with vegetation growth to discuss the characteristics of an ideal index for different forest change and monitoring purposes. The simplified time series curves for different indices are shown in Figure 2.

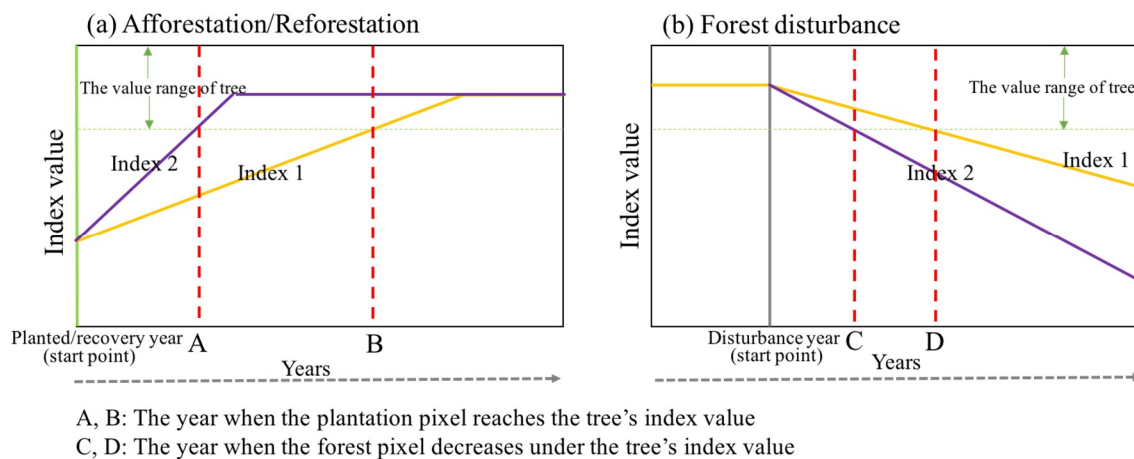


Figure 2. Simplified time series of different indices used for the study of forest change.

Figure 2 shows two kinds of indices. One, as in Index 2, has a fast response to vegetation change. The other, as in Index 1 has a relatively slow response and change trend. In Figure 2a, Index 2 reaches the spectral index value of tree faster than Index 1. The value range for forest will be defined in the following section. Index 2 is more sensitive to vegetation growth but saturates quickly. By contrast, Index 1 has a more gradual pattern and takes longer to reach saturation. It can provide a longer period of information on the sapling growth process and matches more closely to the length of the plantation

growth. Thus, Index 1 is more suitable for describing sapling growth. In other words, the ideal index for sapling growth monitoring is the one that takes longer to saturate with a slower change trend and longer time from the planting year to the year when the sapling meets the spectral index value of tree.

Detecting the actual area of afforestation requires a different index. The traditional method for estimating an afforestation area relies on on-site visits. It takes three field visits over three consecutive years to determine the area of afforestation [42]. However, this method is subjective and time-consuming. Additionally, there is a tendency for both local government and participating farmers to report a larger afforestation area in order to obtain more compensation money from central government [9]. Meanwhile, it is difficult to distinguish forest plantations at early stages of growth from other land cover types. A central government needs to obtain accurate information on the actual areas of plantation as quickly as possible. For this purpose, Index 2 can be used to determine the afforestation area sooner than Index 1. Therefore, Index 2 is more desirable for monitoring afforestation.

For monitoring gradual forest disturbance, it is crucial to get accurate disturbance information as quickly as possible. Therefore, Index 2 would also be useful to monitor forest disturbance.

3.4. Calculating the Year When Saplings from Afforestation were Recognized as Forest

Since the objective of this study is to assess the potential of various spectral indices in evaluating afforestation, we only focus on afforestation areas (areas from non-forest to forest). Finding out how many years the saplings take to mature as forest in different spectral indices is a direct way to evaluate afforestation and growth in these indices. However, newly planted saplings are usually hard to distinguish from other vegetation types. This makes it difficult to accurately obtain the precise year the saplings were planted by participating farmers. In this study, we calculated the year when the saplings from afforestation were recognized as forest by different spectral indices.

We first generated afforestation maps from 1997 to 2010. Then, a comparison among the eighteen spectral indices was carried out on all the obtained afforestation pixels. The afforestation area was obtained using the method developed in a previous study [9] and the method of vegetation change tracker (VCT) [29]. We chose the united results from both methods.

Additionally, most of the GGP was implemented on steep slopes. Croplands are usually located at low elevations and on flat ground. Therefore, Digital Elevation Model (DEM) data was used to modify the afforestation results. The DEM is SRTM30 (near-global digital elevation model comprising a combination of data from Shuttle Radar Topography Mission, downloaded from <https://earthexplorer.usgs.gov>). With the help of interpretation and Google Earth images, we masked out non-afforestation pixels caused by cropland, undetected clouds, cloud shadow or other noises to ensure the accuracy of obtained afforestation pixels. For validation, we collected 930 afforestation sample points (Figure 1) in all eleven Landsat scenes according to a stratified sampling scheme. Visual interpretation based on high-resolution historical images in Google Earth (for this area, the high resolution images in Google Earth are mostly Quickbird images) and time series Landsat images were used to label these test sample pixels. The overall accuracy was 92% (Table 2).

In this study, we used the dark object method [43] to generate forest samples for each year separately to reduce possible influences caused by images in different years. Moreover, the land cover map of 2010 [23] was used to mask out non-forest areas in the annual forest sample set. Using the forest sample in each year to calculate a mean and a standard deviation value of forest, we determined that if the index value of an afforestation pixel fell within the range ± 1.96 standard deviation to the mean, the plantation pixel could be recognized as forest. If the afforestation pixel was recognized as forest, the pixel in that year was set to 1, otherwise, it was set to 0. Since, we accepted as afforestation area all the land cover changes from non-forest into forest and discarded all areas where the land cover change was from forest into non-forest, once the plantation matured as forest, the process was not reversible during the period from 1997 to 2010. With this basic rule, we filtered those afforestation results using a temporal consistency check method [44] to generate the final results of the year when saplings from afforestation were recognized as forest. This was done for each of the eighteen spectral indices.

Table 2. Summary of correctly identified afforestation sample pixels.

Class	Reference of Afforestation Truth Pixels												Total
	125033	125034	125035	125036	126033	126034	126035	126036	127035	127036	128036	Other	
125033 afforestation	80	0	0	0	0	0	0	0	0	0	0	9	89
125034 afforestation	0	76	0	0	0	0	0	0	0	0	0	8	84
125035 afforestation	0	0	46	0	0	0	0	0	0	0	0	6	52
125036 afforestation	0	0	0	88	0	0	0	0	0	0	0	5	93
126033 afforestation	0	0	0	0	65	0	0	0	0	0	0	10	75
126034 afforestation	0	0	0	0	0	94	0	0	0	0	0	6	100
126035 afforestation	0	0	0	0	0	0	93	0	0	0	0	3	96
126036 afforestation	0	0	0	0	0	0	0	36	0	0	0	5	41
127035 afforestation	0	0	0	0	0	0	0	0	93	0	0	7	100
127036 afforestation	0	0	0	0	0	0	0	0	0	94	0	6	100
128036 afforestation	0	0	0	0	0	0	0	0	0	0	92	8	100
total	80	76	46	88	65	94	93	36	93	94	92	73	930

4. Results

Because it is usually difficult to obtain an accurate year when participating farmers plant saplings, instead of getting the exact years of all the afforestation pixels needed to fall into the forest range, we calculated the time when these afforestation pixels would reach the forest stage based on the above method. Then, we counted the cumulative percentage of the afforestation area that matured as forest in each year for each of the eighteen indices from 1999 to 2010, during the Green for Grain Project period. The cumulative percentage reaching 100% faster indicates that the index took a shorter time to detect the afforestation pixels as forest. At the same year, a higher cumulative percentage implies a relatively faster trend detected by the index.

Here we show the summarized results of all eleven Landsat scenes and the top five Landsat scenes with the greatest afforestation area (Figure 3). It can be seen that, under the same conditions, different spectral indices have different capabilities in characterizing the process of afforestation. The increased trend varies differently among these eleven indices.

Tasseled Cap Greenness (TCG) performs differently compared with the remaining indices. TCG indicated there were over 40% afforestation pixels of mature forest in 1999. This does not agree with fact. The Grain for Green project only started in 1999, and the new plantations were only small saplings. There is a high possibility that TCG cannot distinguish forest from other vegetation types such as cropland and shrubland. Therefore, in the subsequent discussions we drop this index.

The results were consistent among the eleven Landsat scenes. Under the same amount of afforestation, the SWIR1 and Tasseled Cap Brightness (TCB) indices show that the cumulative percentage of forest area maturing from the same afforestation reaches 100% earlier and is relatively higher at each year than the remaining indices. This means these two indices took the shortest time to detect the afforestation pixels as forest. The Wetness Brightness Difference Index (WBDI) is in the second tier. Soil Adjusted Vegetation Index (SAVI), Normalized Difference Vegetation Index (NDVI), Tasseled-Cap Angle (TCA), Atmospherically Resistant Vegetation Index (ARVI), Normalized Burned ratio(NBR), Normalized Burned ratio2 (NBR2), and Disturbance Index(DI) are quite similar. They hold the lowest cumulative percentage in every year and the longest time for all the afforestation.

(a) All eleven Landsat scenes

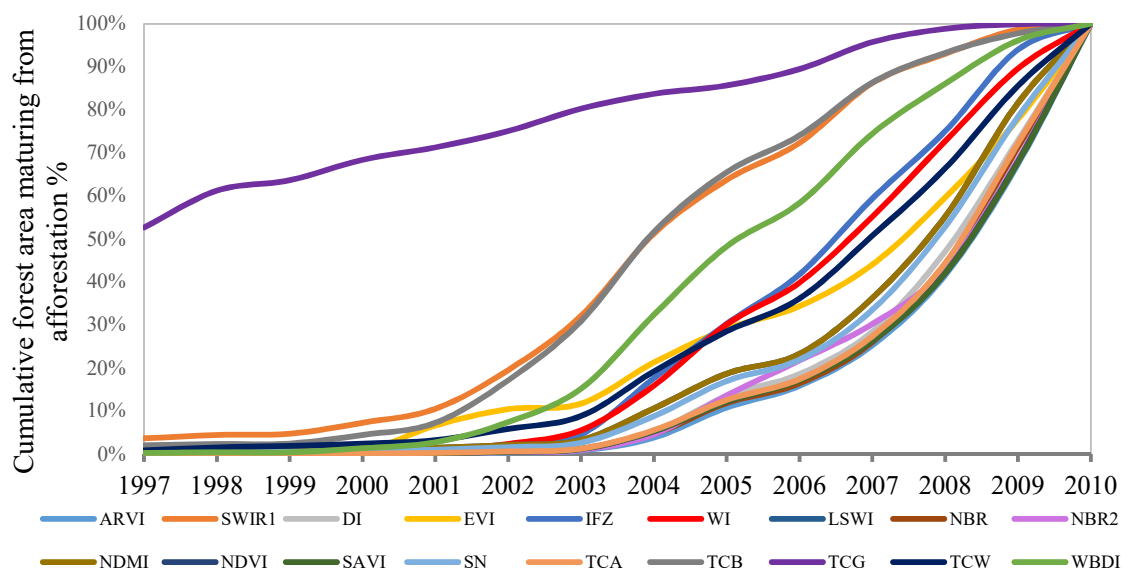
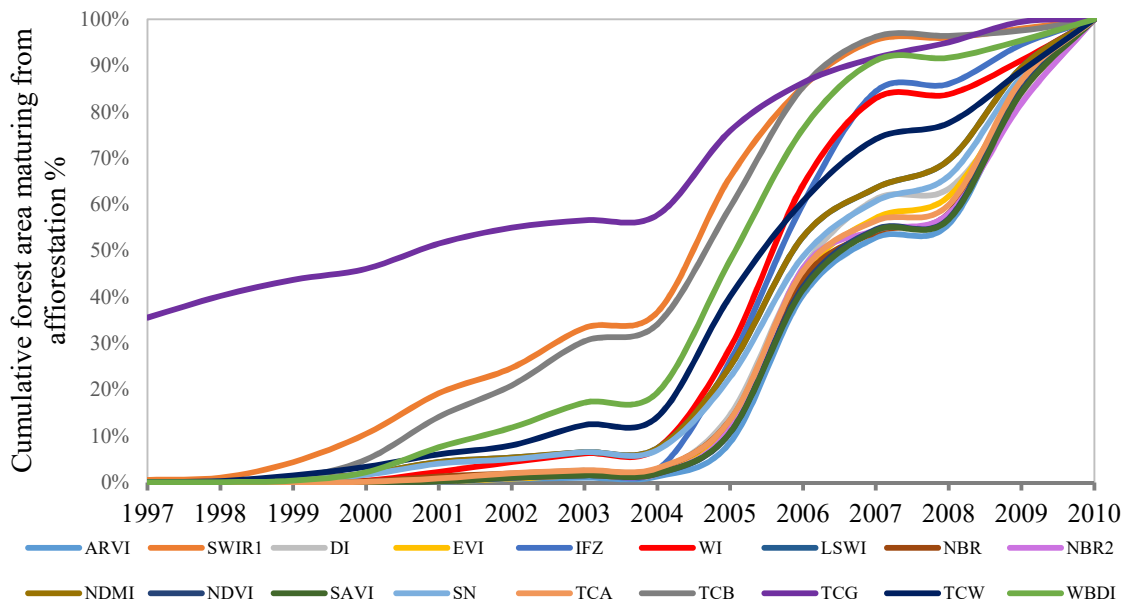


Figure 3. Cont.

(b) path/row : 127/35



(c) path/row:128/36

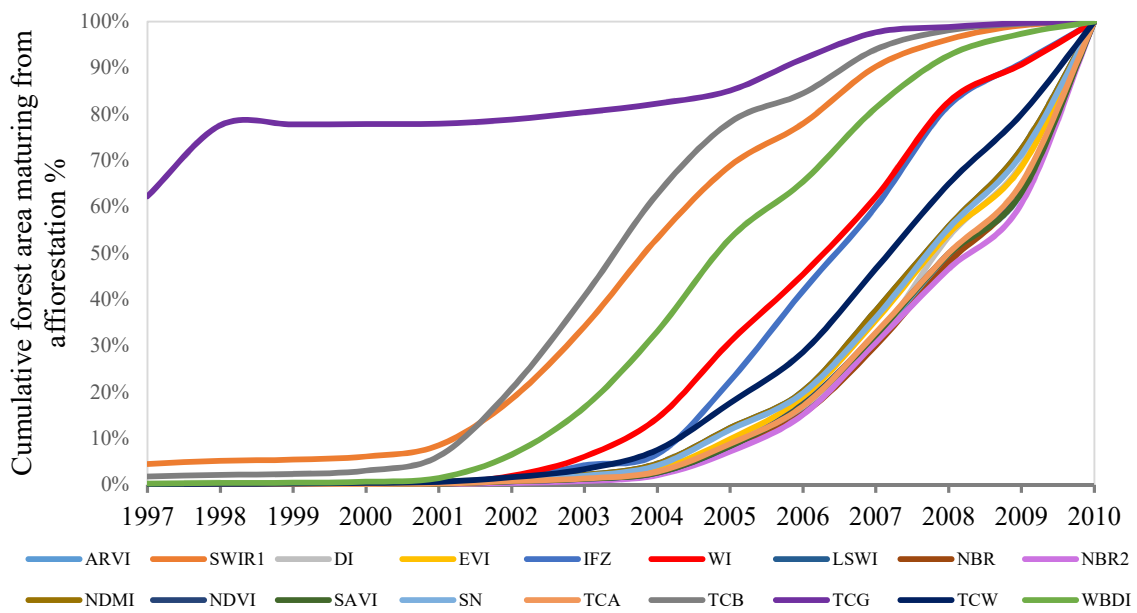
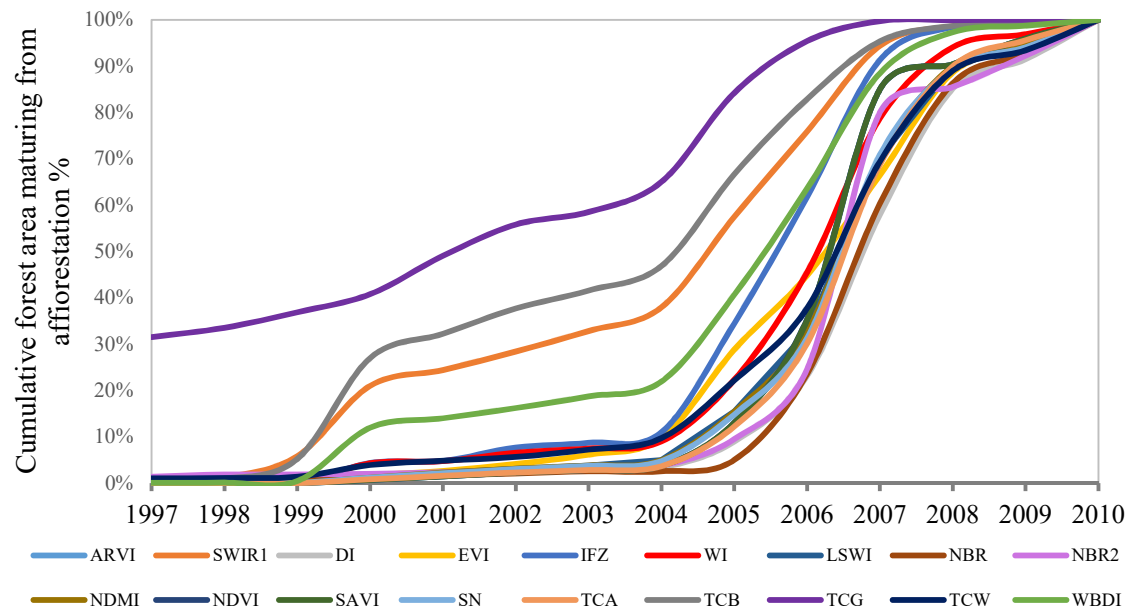


Figure 3. Cont.

(d) path/row : 127/36



(e) path/row : 126/34

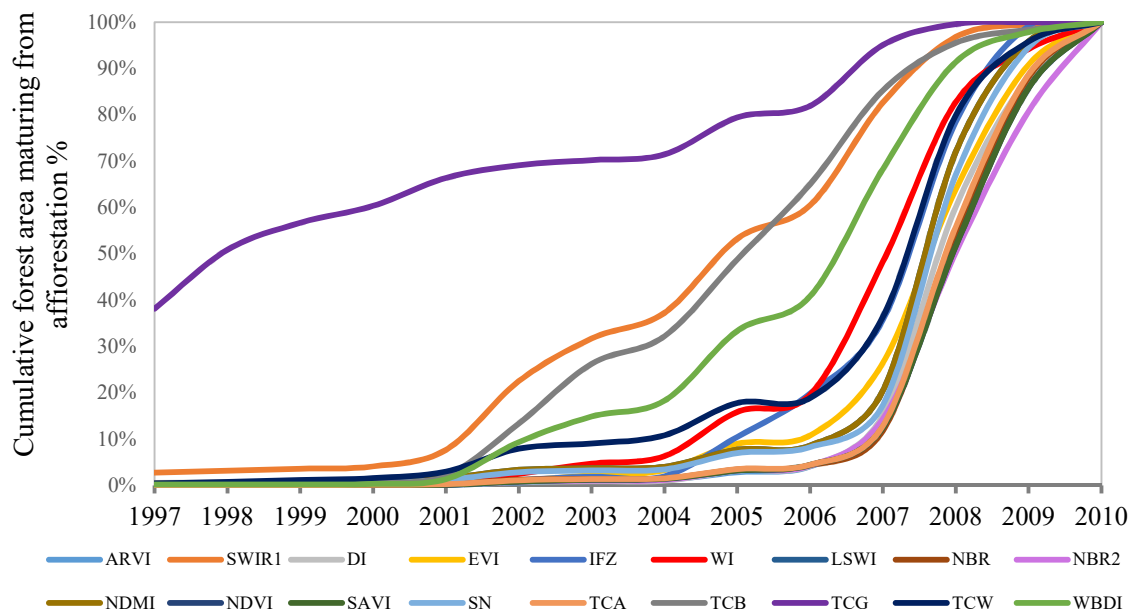


Figure 3. Cont.

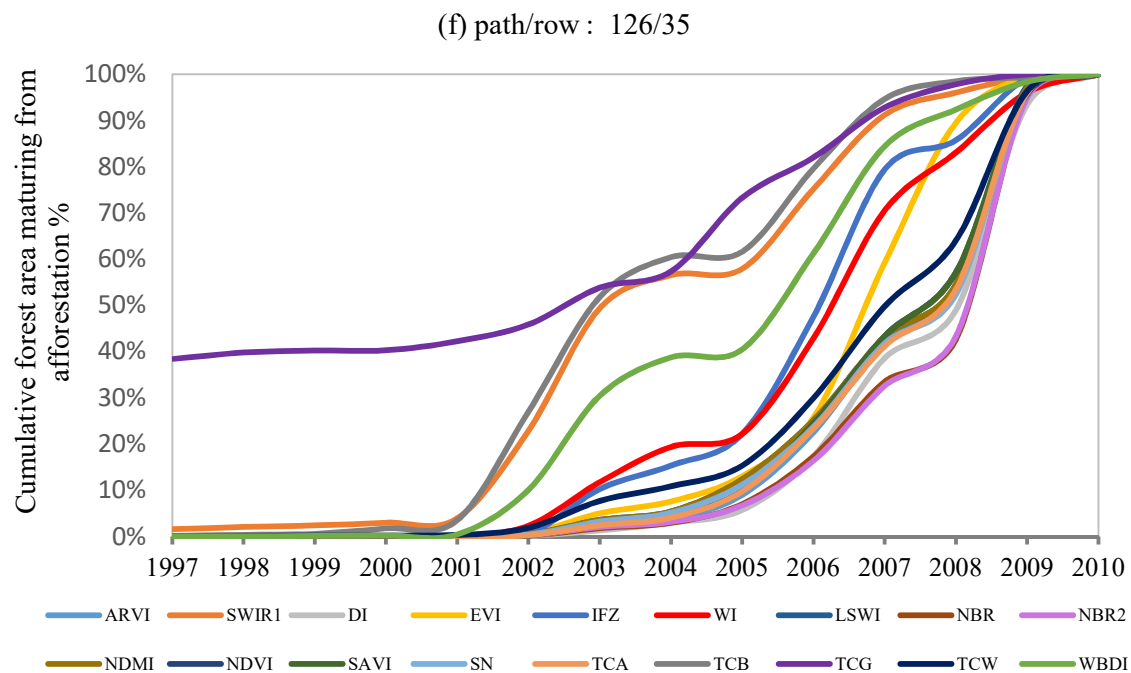


Figure 3. Cumulative percentage of afforestation area maturing into forest in each year for typical Landsat scenes. ((a) Results for all eleven Landsat scenes; (b–f) Results for different Landsat scenes).

5. Discussion

In order to analyze and prove our results, we randomly chose 147 afforestation sample pixels (Figure 1) and visually interpreted them with the help of high-resolution historical Google Earth images (mostly Quickbird images) and Landsat time series data to determine the year of plantation. We used these afforestation samples with the planted year information to estimate exactly how many years the saplings needed to grow to meet the forest threshold value for each index. The results are shown in Figure 4.

The results of Figure 4 are quite similar to Figure 3. TCB and SWIR1 are similar and they took the shortest time to identify afforestation as forest. They both showed great sensitivity to green vegetation. They are in accordance with the characteristics of the best index for detecting the actual afforestation area. As mentioned above, due to the incomplete compensation policy and development requirement of local governments, some afforestation areas have been converted back to their former land use types or converted to construction land. The shorter than 5-year capability of the SWIR1 and TCB indices to identify afforestation allows for prompt detection of over-reporting and destruction of afforestation. Furthermore, TCB and SWIR1 may be helpful for forest disturbance monitoring, especially in cases of disease, infestation, or drought. Often these disturbances are not detected until the damage reaches a serious state. It would be better to capture the disturbance as soon as the disease or infestation first breaks out so that protective action can be taken in time and damage can be minimized. Additionally, these indices can be helpful for illegal forest thinning.

It takes more than seven years for the NDVI, TCA, NBR, NBR2, SAVI, and DI methods to identify when saplings have converted into forest. The longer duration of information on various stages of afforestation before saplings reach forest can provide more detail on afforestation progress and influence on the environment. This is helpful for continuous monitoring of the growth of saplings during the period of compensation. A comprehensive and full assessment of the achievements and effectiveness of afforestation at different stages can benefit from the types of index that do not saturate quickly. They meet the ideal sapling growth index requirements. Therefore, NBR, NBR2, and DI are more suitable for characterizing the process of plantation growth and different afforestation stages.

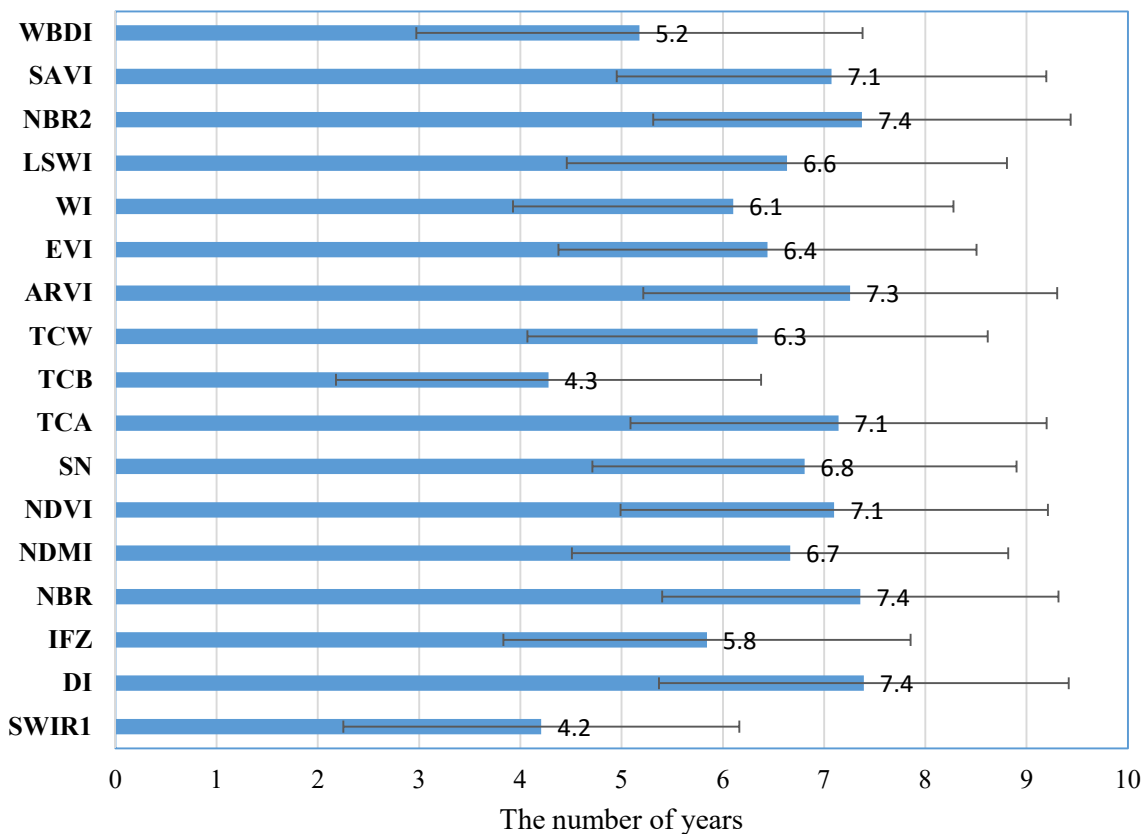


Figure 4. The average time to identify afforestation as forest by different spectral indices.

Additionally, reforestation is quite similar to afforestation. They are both gradual forest changes. Those indices suitable for monitoring afforestation can also be applied to monitoring the process of forest recovery. Pickell et al. only compared SWIR1, TCG, NDVI, and NBR to estimate forest recovery. They found that NBR took the longest mean year to recover and TCG took the shortest [19]. Frazier et al. used trajectories of all tasseled cap indices to understand the forest recovery process and found that tasseled cap wetness (TCW) contained more detail on vegetation structure and growth [17]. Their results are similar to ours to some extent, as the ranking of various spectral indices is similar, but different in plantation or recovery growth trend for the same index. The results of the same index can vary greatly under different conditions and location. They can be influenced by temperature, moisture and other geographical conditions. The plantation of different species can also mean different results. Indices for studying forest change dynamics should be analyzed for each specific region. Our results can be used to provide guidance in semi-arid areas in other parts of the world.

6. Conclusions

We assessed the potential of eighteen spectral indices in determining the earliest year when afforestation can be identified. We also compared their capability in characterizing afforestation growth processes at various stages. The results indicate that under the same conditions, different spectral indices have different sensitivity and capability in characterizing afforestation processes.

DI, NBR, and NBR2 took longer to saturate when monitoring the process of newly planted saplings turning into matured forest during afforestation, which provide a capability to distinguish different sapling growth stages. Additionally, these indices showed the slowest sapling growth trend, taking about 7.4 years on average to detect forest from saplings. This matches well with the compensation duration of 5–8 years. It can help improve our understanding of sapling growth condition and provide more information during and after the period of government subsidies. Meanwhile, it allows us to better evaluate the achievement of various stages of afforestation during the 10-year Green for Grain

program (1999–2010). These indices are the most suitable indices for continuously monitoring the progress of sapling growth. Conversely, SWIR1 and TCB showed great sensitivity to green vegetation and saturated quickly with the growing vegetation. These indices can be applied to find cases of over-reporting of afforestation and for early detection of forest disturbance. Moreover, these can help monitor the loss of land due to reversal of afforestation. Through careful selection of spectral indices and monitoring using satellite remote sensing, the government can more precisely adjust subsidies according to the process of sapling growth to help relieve the concerns of participating farmers and protect afforestation from being destroyed.

Author Contributions: J.G. did the analysis, drafted the paper. P.G. revised the paper.

Funding: This research is partially supported by Meteorological Public Benefit project of China (GYHY201506010).

Acknowledgments: The authors acknowledge Pauline Lovell and Arthur Cracknell for their kind help and comments on this paper.

Conflicts of Interest: The authors declare no conflict of interest.

References

1. The Food and Agriculture Organization of the United Nations. *Global Forest Resources Assessment 2015*; The Food and Agriculture Organization of the United Nations: Rome, Italy, 2015.
2. Shen, R.M. Forestry Policy New Deal in China: Policy Process and Effect. Ph.D. Thesis, Tsinghua University, Beijing, China, 2014.
3. The State Forestry Administration of the People's Republic of China. *China Forest Resources Report (2009–2013)*; China Forestry Publishing House: Beijing, China, 2014.
4. Ministry of Ecology and Environment of People's Republic of China. *China Environmental Status Bulletin 2014*; Ministry of Ecology and Environment of People's Republic of China: Beijing, China, 2015.
5. Liu, S.; Gong, P. Change of surface cover greenness in china between 2000 and 2010. *Chin. Sci. Bull.* **2012**, *57*, 2835–2845. [[CrossRef](#)]
6. Liu, J.; Li, S.; Ouyang, Z.; Tam, C.; Chen, X. Ecological and socioeconomic effects of china's policies for ecosystem services. *Proc. Natl. Acad. Sci. USA* **2008**, *105*, 9477–9482. [[CrossRef](#)] [[PubMed](#)]
7. Wang, X.; Catt, S.; Pangestu, M.; Temple-Smith, P. Impact of china's grain for green project on the landscape of vulnerable arid and semi-arid agricultural regions: A case study in northern shaanxi province. *J. Appl. Ecol.* **2009**, *46*, 536–543.
8. Cao, S.X.; Xu, C.G.; Li, C.; Wang, X.Q. Attitudes of farmers in china's northern shaanxi province towards the land-use changes required under the grain for green project, and implications for the project's success. *Land Use Policy* **2009**, *26*, 1182–1194. [[CrossRef](#)]
9. Guo, J.; Gong, P. *Forest Cover Dynamics from Landsat Time-Series Data over Yan'an City on the Loess Plateau during the Grain for Green Project*; Taylor & Francis, Inc.: Abingdon, UK, 2016; pp. 4101–4118.
10. Hansen, M.C.; Potapov, P.V.; Moore, R.; Hancher, M.; Turubanova, S.A.; Tyukavina, A.; Thau, D.; Stehman, S.V.; Goetz, S.J.; Loveland, T.R. High-resolution global maps of 21st-century forest cover change. *Science* **2014**, *342*, 850–853. [[CrossRef](#)] [[PubMed](#)]
11. Huang, H.; Chen, Y.; Clinton, N.; Wang, J.; Wang, X.; Liu, C.; Gong, P.; Yang, J.; Bai, Y.; Zheng, Y. Mapping major land cover dynamics in beijing using all landsat images in google earth engine. *Remote Sens. Environ.* **2017**. [[CrossRef](#)]
12. Banskota, A.; Kayastha, N.; Falkowski, M.J.; Wulder, M.A.; Froese, R.E.; White, J.C. Forest monitoring using landsat time series data: A review. *Can. J. Remote Sens.* **2014**, *40*, 362–384. [[CrossRef](#)]
13. Cohen, W.B.; Healey, S.P.; Yang, Z.; Stehman, S.V.; Brewer, C.K.; Brooks, E.B.; Gorelick, N.; Huang, C.; Hughes, M.J.; Kennedy, R.E. How similar are forest disturbance maps derived from different landsat time series algorithms? *Forests* **2017**, *8*, 98. [[CrossRef](#)]
14. Vogelmann, J.E.; Gallant, A.L.; Shi, H.; Zhu, Z. Perspectives on monitoring gradual change across the continuity of landsat sensors using time-series data. *Remote Sens. Environ.* **2016**, *185*, 258–270. [[CrossRef](#)]
15. Chu, T.; Guo, X.; Takeda, K. Remote sensing approach to detect post-fire vegetation regrowth in siberian boreal larch forest. *Ecol. Indic.* **2016**, *62*, 32–46. [[CrossRef](#)]

16. Cuevasgonzález, M.; Gerard, F.; Balzter, H.; Riaño, D. Analysing forest recovery after wildfire disturbance in boreal siberia using remotely sensed vegetation indices. *Glob. Chang. Biol.* **2010**, *15*, 561–577. [[CrossRef](#)]
17. Frazier, R.J.; Coops, N.C.; Wulder, M.A. Boreal shield forest disturbance and recovery trends using landsat time series. *Remote Sens. Environ.* **2015**, *170*, 317–327. [[CrossRef](#)]
18. Hais, M.; Jonášová, M.; Langhammer, J.; Kučera, T. Comparison of two types of forest disturbance using multitemporal landsat tm/etm+ imagery and field vegetation data. *Remote Sens. Environ.* **2009**, *113*, 835–845. [[CrossRef](#)]
19. Pickell, P.D.; Hermosilla, T.; Frazier, R.J.; Coops, N.C.; Wulder, M.A. Forest recovery trends derived from landsat time series for north american boreal forests. *Int. J. Remote Sens.* **2016**, *37*, 138–149. [[CrossRef](#)]
20. Schroeder, T.A.; Wulder, M.A.; Healey, S.P.; Moisen, G.G. Mapping wildfire and clearcut harvest disturbances in boreal forests with landsat time series data. *Remote Sens. Environ.* **2011**, *115*, 1421–1433. [[CrossRef](#)]
21. Jian, S.; Zhao, C.; Fang, S.; Yu, K. Effects of different vegetation restoration on soil water storage and water balance in the chinese loess plateau. *Agric. For. Meteorol.* **2015**, *206*, 85–96. [[CrossRef](#)]
22. Gong, P.; Wang, J.; Yu, L.; Zhao, Y.; Zhao, Y.; Liang, L.; Niu, Z.; Huang, X.; Fu, H.; Liu, S. Finer resolution observation and monitoring of global land cover: First mapping results with landsat tm and etm+ data. *Int. J. Remote Sens.* **2013**, *34*, 2607–2654. [[CrossRef](#)]
23. Li, C.; Wang, J.; Hu, L.; Yu, L.; Clinton, N.; Huang, H.; Yang, J.; Gong, P. A circa 2010 thirty meter resolution forest map for china. *Remote Sens.* **2014**, *6*, 5325–5343. [[CrossRef](#)]
24. White, J.C.; Wulder, M.A.; Hobart, G.W.; Luther, J.E.; Hermosilla, T.; Griffiths, P.; Coops, N.C.; Hall, R.J.; Hostert, P.; Dyk, A. Pixel-based image compositing for large-area dense time series applications and science. *Can. J. Remote Sens.* **2014**, *40*, 192–212. [[CrossRef](#)]
25. Savitzky, A.; Golay, M.J.E. Smoothing and differentiation of data by simplified least squares procedures. *Anal. Chem.* **1964**, *36*, 1627–1639. [[CrossRef](#)]
26. Kennedy, R.E.; Cohen, W.B.; Schroeder, T.A. Trajectory-based change detection for automated characterization of forest disturbance dynamics. *Remote Sens. Environ.* **2007**, *110*, 370–386. [[CrossRef](#)]
27. Crist, E.P.; Kauth, R.J. The tasseled cap de-mystified. *Photogramm. Eng. Remote Sens.* **1986**, *52*, 81–86.
28. Healey, S.P.; Cohen, W.B.; Yang, Z.; Krankina, O.N. Comparison of tasseled cap-based landsat data structures for use in forest disturbance detection. *Remote Sens. Environ.* **2005**, *97*, 301–310. [[CrossRef](#)]
29. Huang, C.Q.; Goward, S.N.; Masek, J.G.; Thomas, N.; Zhu, Z.L.; Vogelmann, J.E. An automated approach for reconstructing recent forest disturbance history using dense landsat time series stacks. *Remote Sens. Environ.* **2010**, *114*, 183–198. [[CrossRef](#)]
30. Vogelmann, J.E.; Tolk, B.; Zhu, Z. Monitoring forest changes in the southwestern united states using multitemporal landsat data. *Remote Sens. Environ.* **2009**, *113*, 1739–1748. [[CrossRef](#)]
31. Vogelmann, J.E.; Xian, G.; Homer, C.; Tolk, B. Monitoring gradual ecosystem change using landsat time series analyses: Case studies in selected forest and rangeland ecosystems. *Remote Sens. Environ.* **2012**, *122*, 92–105. [[CrossRef](#)]
32. Key, C.H.; Benson, N.C. *Landscape Assessment: Ground Measure of Severity, the Composite Burn Index; and Remote Sensing of Severity, the Normalized Burn Ratio*; USDA Forest Service: Ogden, UT, USA, 2006; pp. 1–51.
33. Storey, E.A.; Stow, D.A.; O’Leary, J.F. Assessing postfire recovery of chamise chaparral using multi-temporal spectral vegetation index trajectories derived from landsat imagery. *Remote Sens. Environ.* **2016**, *183*, 53–64. [[CrossRef](#)]
34. Goodwin, N.R.; Coops, N.C.; Wulder, M.A.; Gillanders, S.; Schroeder, T.A.; Nelson, T. Estimation of insect infestation dynamics using a temporal sequence of landsat data. *Remote Sens. Environ.* **2008**, *112*, 3680–3689. [[CrossRef](#)]
35. Kaufman, Y.J.; Tanré, D. Atmospherically resistant vegetation index (arvi) for eos-modis. *IEEE Trans. Geosci. Remote Sens.* **1992**, *30*, 261–270. [[CrossRef](#)]
36. Kou, W.; Liang, C.; Wei, L.; Hernandez, A.; Yang, X. Phenology-based method for mapping tropical evergreen forests by integrating of modis and landsat imagery. *Forests* **2017**, *8*, 34. [[CrossRef](#)]
37. Lehmann, E.A.; Wallace, J.F.; Caccetta, P.A.; Furby, S.L.; Zdunic, K. Forest cover trends from time series Landsat data for the Australian continent. *Int. J. Appl. Earth Obs. Geoinf.* **2013**, *21*, 453–462. [[CrossRef](#)]
38. Sonnenschein, R.; Kuemmerle, T.; Udelhoven, T.; Stellmes, M.; Hostert, P. Differences in landsat-based trend analyses in drylands due to the choice of vegetation estimate. *Remote Sens. Environ.* **2011**, *115*, 1408–1420. [[CrossRef](#)]

39. Helmer, E.H.; Lefsky, M.A.; Roberts, D.A. Biomass accumulation rates of Amazonian secondary forest and biomass of old-growth forests from Landsat time series and the Geoscience Laser Altimeter System. *J. Appl. Remote Sens.* **2009**, *3*, 201–210.
40. Chen, Y.; Liu, H.; Meng, X. *System of Monitoring and Management for the State Key Forestry Ecological Project*; China Forestry Publishing House: Beijing, China, 2011.
41. National Development and Reform Commission. Available online: http://www.ndrc.gov.cn/zcfb/jd/201409/t20140927_679119.html (accessed on 17 September 2018).
42. General Administration of Quality Supervision, Inspection and Quarantine of the People's Republic of China. *Checking Regulation in Project for Conversion of Cropland to Forest (gb/t 23231-2009)*; China Forestry Publishing House: Beijing, China, 2009.
43. Huang, C.; Song, K.; Kim, S.; Townshend, J.R.G.; Davis, P.; Masek, J.G.; Goward, S.N. Use of a dark object concept and support vector machines to automate forest cover change analysis. *Remote Sens. Environ.* **2008**, *112*, 970–985. [[CrossRef](#)]
44. Li, X.; Gong, P.; Liang, L. A 30-year (1984–2013) record of annual urban dynamics of Beijing city derived from Landsat data. *Remote Sens. Environ.* **2015**, *166*, 78–90. [[CrossRef](#)]



© 2018 by the authors. Licensee MDPI, Basel, Switzerland. This article is an open access article distributed under the terms and conditions of the Creative Commons Attribution (CC BY) license (<http://creativecommons.org/licenses/by/4.0/>).